Supporting Information

Transformable Nanostructures of Platinum-Containing Organosilane Hybrids: Non-covalent Self-Assembly of Polyhedral Oligomeric Silsesquioxanes Assisted by Pt···Pt and π–π Stacking Interactions of Alkynylplatinum(II) Terpyridine Moieties

Ho-Leung Au-Yeung, Sammual Yu-Lut Leung, Anthony Yiu-Yan Tam, Vivian Wing-Wah Yam*

Institute of Molecular Functional Materials (Areas of Excellence Scheme, University Grants Committee (Hong Kong)) and Department of Chemistry, The University of Hong Kong, Pokfulam Road, Hong Kong

Materials and Reagents. Potassium tetrachloroplatinate(II) ($K_2[PtCl_4]$) (Chem. Pur.), octavinyl POSS (Hybrid Plastic Inc.), phenylacetylene (Sigma-Aldrich Co. Ltd.), and triethylamine (Apollo Scientific Ltd.) were obtained from the corresponding chemical company. Monohydroxyl-functionalized heptavinyl POSS (VPOSS−OH)[1] and 4'-carboxyphenyl-2,2':6',2''-terpyridine[2] were synthesized according to literature methods. Tetrahydrofuran (Acros Organics Co. Ltd., spectroscopic grade) were used for spectroscopic studies without further purification. All other reagents, unless otherwise specified, were of analytical grade and were used as received without further purification.

Physical Measurements and Instrumentation. ^{1}H NMR spectra were recorded on a Bruker AVANCE 300 or 400 (300 and 400 MHz) NMR spectrometer. $^{13}C\{^{1}H\}$ NMR spectra were recorded on a Bruker AVANCE 500 (125.7 MHz) NMR spectrometer. Positive-ion FAB mass spectra were recorded on a Thermo Scientific DFS high resolution magnetic sector mass spectrometer. IR spectra were obtained as KBr disk on a Bio-Rad FTS-7 Fourier transform infrared spectrophotometer (4000–400 cm^{-1}). Elemental analyses of the complexes were performed on a Flash EA 1112 elemental analyzer at the Institute of Chemistry, Chinese Academy of Sciences. The UV–visible spectra were obtained using a Hewlett-Packard 8452A diode array spectrophotometer. Emission spectra at room temperature were recorded on a Spex Fluorolog-3 model FL3-211 fluorescence spectrofluorometer equipped with an R2658P PMT detector. Transmission electron microscopy (TEM) experiments were performed on a Philips CM100 Transmission Electron Microscope with an accelerating voltage of 200 kV. Scanning electron

microscopy (SEM) experiments were performed on a Hitachi S4800 FEG operating at 4.0-6.0 kV. The samples for TEM and SEM were prepared by drop casting dilute solutions onto a carbon coated copper grid and silicon wafer respectively, which was then allowed to undergo slow evaporation of the solvents in air for 10 minutes to remove any excess solvent. Topographical images and phase images of atomic force micrographs (AFM) were collected on an Asylem MFP3D atomic force microscope with ARC2 SPM Controller under constant temperature and atmospheric pressure. Samples were prepared by drop casting dilute solutions onto a silicon wafer. Dynamic light scattering was measured with Malvern (UK) Zetasizer Nano ZS with internal HeNe laser (632.8 nm) at room temperature.

Synthesis and characterization

Synthesis

The synthetic route for complex **1** is shown in Scheme S1. All reactions, unless otherwise specified, were carried out under an inert atmosphere of nitrogen using standard Schlenk techniques.

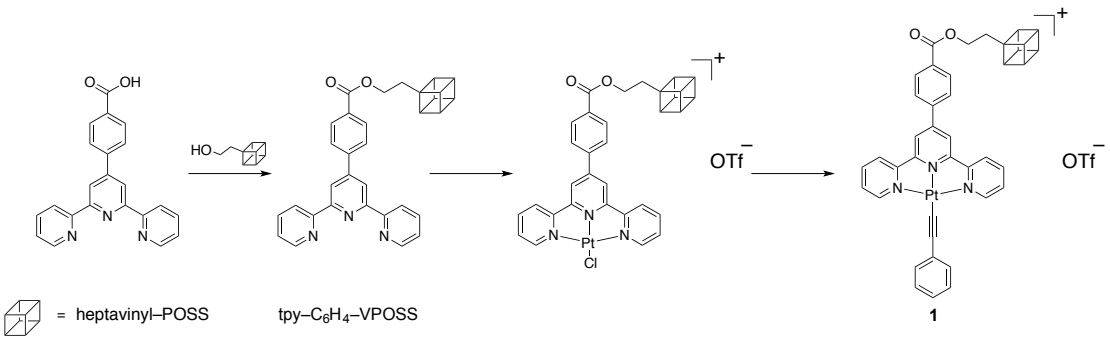

Scheme S1. Synthetic route for Complex **1**.

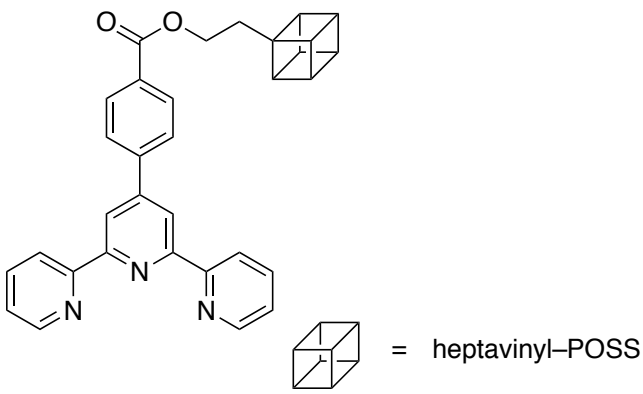

VPOSS–phenyl–terpyridine (tpy–C_6H_4–VPOSS): 4'-Carboxyphenyl-2,2':6',2''-terpyridine (125 mg, 0.36 mmol), VPOSS−OH (200 mg, 0.30 mmol), EDC•HCl (235 mg, 1.22 mmol) and 4-dimethylaminopyridine (DMAP) (40 mg, 0.33 mmol) were dissolved in dichloromethane (200 ml). The resulted mixture was stirred at ambient temperature for 24 h, after which the mixture was evaporated to dryness. The residue was further purified by column chromatography using dichloromethane followed by dichloromethane–acetone (10:1 v/v) as eluent to afford pure tpy–C_6H_4–VPOSS as a white solid. Yield: 60 mg, 0.061 mmol, 20 %. ^{1}H NMR (300 MHz, $CDCl_3$, 298 K, relative to Me_4Si): δ 1.40 (t, 2H, J = 8.0 Hz, –CH_2–Si), 4.53 (t, 2H, J = 8.0, O–CH_2–), 5.84–6.16 (m, 21H, Si–HC=CH_2), 7.38 (t, 2H, J = 6.2 Hz, tpy), 7.88–7.95 (m, 4H, –C_6H_4– and tpy), 8.18 (d, 2H, J = 8.3 Hz, –C_6H_4–), 8.68–8.76 (m, 6H, tpy). Positive FAB-MS: m/z: 986 $[M + H]^+$. IR (KBr) : v = 1111 cm^{-1} (Si–O). Anal. Found (%): C, 45.73; H, 4.06; N, 4.22. Calcd for tpy–C_6H_4–VPOSS•MeOH: C, 45.99; H, 4.26; N, 4.13.

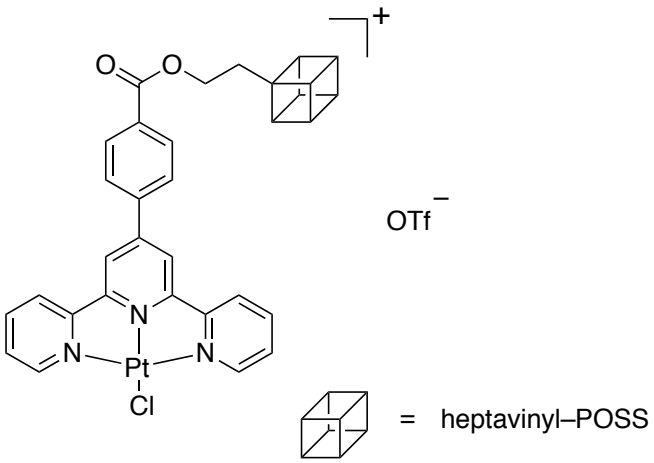

[Pt(tpy–C_6H_4–VPOSS)Cl]OTf: The chloroplatinum(II) precursor complex was prepared according to a modified literature method for the synthesis of chloroplatinum(II) terpyridine complexes[3] using tpy–C_6H_4–VPOSS instead of terpyridine. AgOTf (70 mg, 0.27 mmol) was added to the suspension of $Pt(PhCN)_2Cl_2$ (100 mg, 0.26 mmol) in acetonitrile. The resultant mixture was then refluxed for 12 h. The solution was then filtered and tpy–C_6H_4–VPOSS (300 mg, 0.30 mmol) was added to the clear solution. The resultant mixture was heated overnight at reflux temperature. The crude product was evaporated to dryness followed by purification with column chromatography using dichloromethane-acetone (3:1 v/v) mixture as eluent to give the precursor complex as a yellow solid. Yield: 240 mg, 0.18 mmol, 70 %. ^{1}H NMR (400 MHz, $CDCl_3$, 298 K, relative to Me_4Si): δ 1.34 (t, 2H, J = 8.7 Hz, –CH_2–Si–), 4.53 (t, 2H, J = 8.7 Hz, O–CH_2–), 5.90–6.16 (m, 21H, Si–HC=CH_2), 7.68 (d, 2H, J = 8.6 Hz, –C_6H_4–), 7.78 (t, 2H, J = 8.0 Hz, tpy), 7.96 (d, 2H, J = 8.6 Hz, –C_6H_4–), 8.41 (t, 2H, J = 8.0 Hz, tpy), 8.55 (s, 2H, tpy), 8.85 (d, 2H, J = 8.0 Hz, tpy), 9.11 (d, 2H, J = 8.0 Hz, tpy). ^{13}C{^{1}H} NMR (125.7 MHz, $CDCl_3$, 298 K, relative to Me_4Si): δ 164.93 (–CO_2–), 158.00, 154.37, 151.65, 142.57, 138.26 (tpy), 137.25, 137.10 (Si–HC=$\underline{C}H_2$), 137.06, 132.65, 130.40 (tpy–Ph),

128.62, 128.61 (Si–H<u>C</u>=CH_2), 128.36, 127.71, 127.30, 121.96 (tpy–Ph), 62.37 (O–CH_2–), 13.30 (–CH_2–Si–). Positive FAB-MS: *m*/*z*: 1216 [M − OTf]$^+$. IR (KBr) : *v* = 1111 cm^{-1} (Si–O). Anal. Found (%): C, 32.86; H, 2.86; N, 2.97. Calcd for [Pt(tpy–C_6H_4–VPOSS)Cl]OTf•CH_2Cl_2: C, 33.11; H, 2.85; N, 2.90.

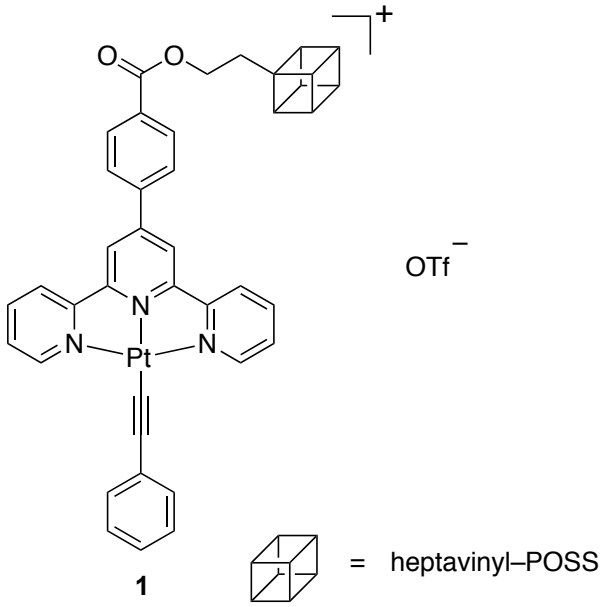

1

[Pt(VPOSS–Ph–tpy)(C≡CC_6H_5)]OTf (1). Complex **1** was prepared according to a modified literature method for the synthesis of alkynylplatinum(II) terpyridine complexes.[4] To a solution of chloroplatinum(II) precursor complex (135 mg, 0.10 mmol) and phenylacetylene (29 mg, 0.29 mmol) in degassed dichloromethane and triethylamine was added a catalytic amount of CuI. The resultant solution was stirred overnight at ambient temperature. The crude product was then purified by column chromatography using dichloromethane-acetone (3:1 v/v) mixture as eluent to give **1** as a dark red solid. Yield: 70 mg, 0.049 mmol, 50 %. ^{1}H NMR (400 MHz, CD_3CN, 330 K, relative to Me_4Si): δ 1.44 (t, 2H, *J* = 7.7 Hz, –CH_2–Si), 4.57 (t, 2H, *J* = 7.7 Hz, O–CH_2–), 5.96–6.19 (m, 21H, Si–CH=CH_2), 7.31 (t, 1H, *J* = 7.5 Hz, –C_6H_5), 7.39 (t, 2H, *J* = 7.5 Hz,

–C_6H_5), 7.57 (d, 2H, *J* = 7.5 Hz, –C_6H_5), 7.85 (t, 2H, *J* = 7.6 Hz, tpy), 8.05 (d, 2H, *J* = 8.5 Hz, –C_6H_4–), 8.27 (d, 2H, *J* = 8.5 Hz, –C_6H_4–), 8.41–8.45 (m, 4H, tpy), 8.55 (s, 2H, tpy), 9.37 (d, 2H, *J* = 7.6 Hz, tpy). $^{13}C\{^1H\}$ NMR (125.7 MHz, [D_8]THF, 298 K, relative to Me_4Si): δ 159.67 (–CO_2–), 155.26, 155.09, 153.20, 142.63 (tpy), 137.67, 137.45 (Si–HC=$\underline{C}H_2$), 137.39, 133.61, 132.92, 131.16, 130.40, 130.33 (tpy–Ph and Ph), 129.69, 129.57 (Si–H$\underline{C}$=CH_2), 129.10, 128.96, 127.92, 127.37, 127.02, 122.69 (tpy–Ph and Ph), 91.43, 83.28 (Pt–C≡C–), 62.13 (O–CH_2–), 14.13 (–CH_2–Si–). Positive FAB-MS: *m/z*: 1282 [M − OTf]$^+$. IR (KBr) : *v* = 1111 cm^{-1} (Si–O), 2120 cm^{-1} (C≡C). Anal. Found (%): C, 37.30; H, 3.10; N, 2.65. Calcd for **1**•$CHCl_3$: C, 37.17; H, 2.92; N, 2.71.

X-Ray crystal structure determination. Single crystals of the chloroplatinum(II) precursor complex suitable for X-ray crystallographic studies was obtained by the diffusion of diethyl ether vapor into a concentrated dichloromethane solution of the complex. The crystal and structure determination data of [Pt(tpy–C_6H_4–VPOSS)Cl]OTf•2CH_2Cl_2 are summarized below. Crystallographic and structural refinement data are given in Table S1. Selected bond lengths and bond angles of the chloroplatinum(II) complex are collected in Table S2. The crystal was mounted in a glass capillary, and the intensity data were collected on a Bruker *ApexII* 1000 CCD diffractometer using graphite-monochromated Cu–Kα radiation (λ = 1.54178 Å). Raw frame data were integrated using the APEX program.[5] Semi-empirical absorption corrections with SADABS[6] were applied. The structures were solved by direct methods employing the SHELXS-97 program[7] and refined by full-matrix least-squares on F^2 using the SHELXL-97 program.[7] In the final stage of least-squares refinement, non-hydrogen atoms of the solvent molecules were refined isotropically; other non-hydrogen atoms were refined anisotropically. Hydrogen atoms were generated by the program SHELXL-97.[7] The positions of hydrogen atoms were calculated on the basis of the riding mode with thermal parameters equal to 1.2 times that of the associated C atoms and participated in the calculation of final R indices.

Table S1 Crystal and structure determination data for the chloroplatinum(II) precursor complex

formula	$C_{38}H_{39}ClN_3O_{14}PtSi_8 \cdot CF_3O_3S \cdot 2(CH_2Cl_2)$
fw	1535.90
a [Å]	9.1551 (1)
b [Å]	9.1571 (1)
c [Å]	35.8168 (5)
α [°]	92.624 (1)
β [°]	91.737 (1)
γ [°]	101.022 (1)
V [Å^3]	2914.85 (6)
Z	2
crystal system	Triclinic
color/habit	Yellow plate crystal
space group	$P\bar{1}$ (No. 2)
D_c [g cm^{-3}]	1.734
T [K]	100 (1)
μ [mm^{-1}]	9.13
F(000)	1528
no. of reflections	17444
no. of independent reflections	9553
R_{int}	0.0411
R_1[a], wR_2[b] ($I > 2(I)$)	0.0605, 0.1594
GoF[c]	1.06

[a] $R_1 = \Sigma ||F_o|-|F_c|| / \Sigma |F_o|$. [b] $wR_2 = [\Sigma w(|F_o^2|-|F_c^2|)^2 / \Sigma w|F_o^2|^2]^{1/2}$.
[c] GoF = $[\Sigma w(|F_o|-|F_c|)^2/(N_{obs}-N_{param})]^{1/2}$.

Table S2 Selected bond distances and angles with estimated standard deviations in parentheses for the chloroplatinum(II) precursor complex

Bond Distances (Å)			
Pt(1)−N(1)	2.005(6)	Pt(1)−N(2)	1.936(5)
Pt(1)−N(3)	2.011(6)	Pt(1)−Cl(1)	2.3111(15)
Bond Angles (deg)			
N(1)−Pt(1)−N(2)	81.3(2)	N(1)−Pt(1)−Cl(1)	99.12(17)
N(2)−Pt(1)−N(3)	80.4(2)	N(2)−Pt(1)−Cl(1)	178.18(18)
N(1)−Pt(1)−N(3)	161.7(2)	N(3)−Pt(1)−Cl(1)	99.08(15)

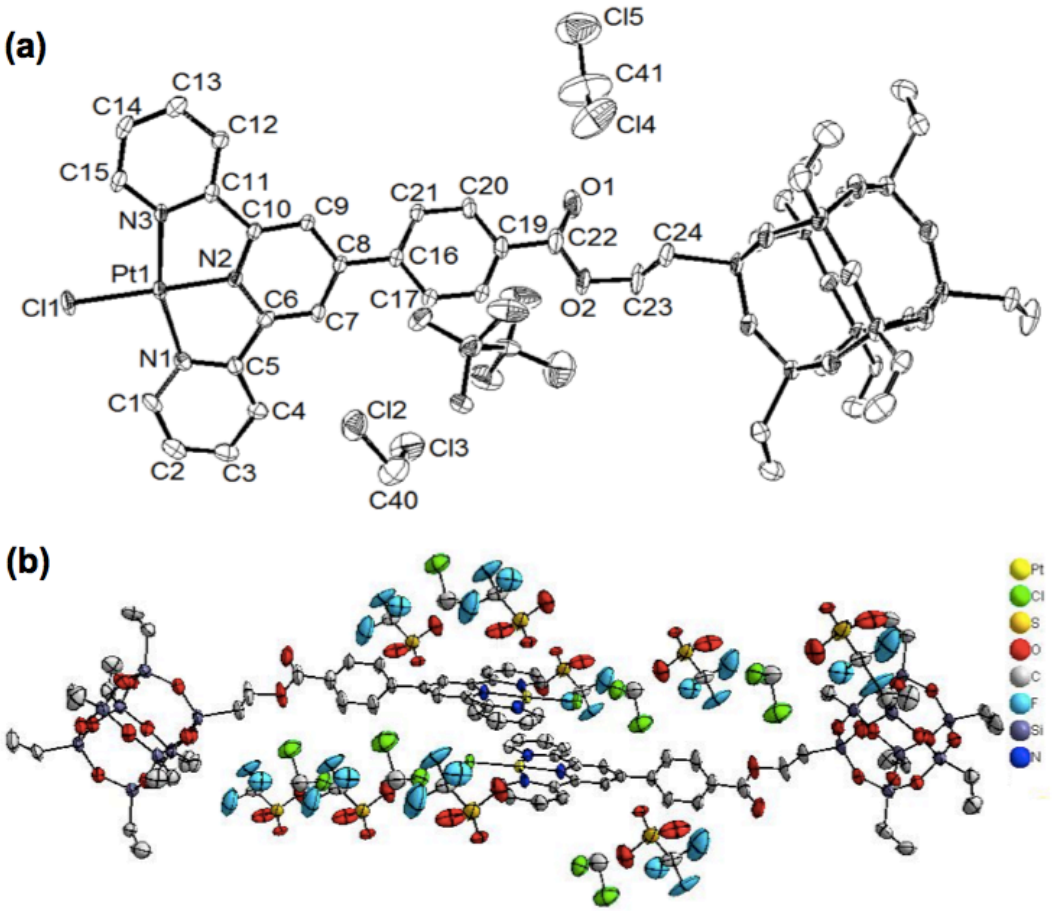

Figure S1. (a) Perspective drawing of the complex cation of [Pt(tpy–C_6H_4–VPOSS)Cl]OTf including solvent molecules and counteranions with atomic numbering. Hydrogen atoms are omitted for clarity. Thermal ellipsoids were shown at the 30% probability level. (b) Crystal-packing diagrams of the complex cations showing a head-to-tail configuration for the dimeric structure together with the position of the counteranions and solvent molecules.

Table S3 Photophysical data of the precursor complex and **1**

Complex	Medium (T / K)	Appearance	Absorption data λ_{max} / nm (ε / $dm^3mol^{-1}cm^{-1}$)
precursor complex	DCM (298)	Yellow	311 (29070), 323 (25720), 338 (22340), 395 (6130), 414 (7890)
1	THF (298)	Yellow	313 (33600), 347 (15560), 430 (7580), 472 (6650)

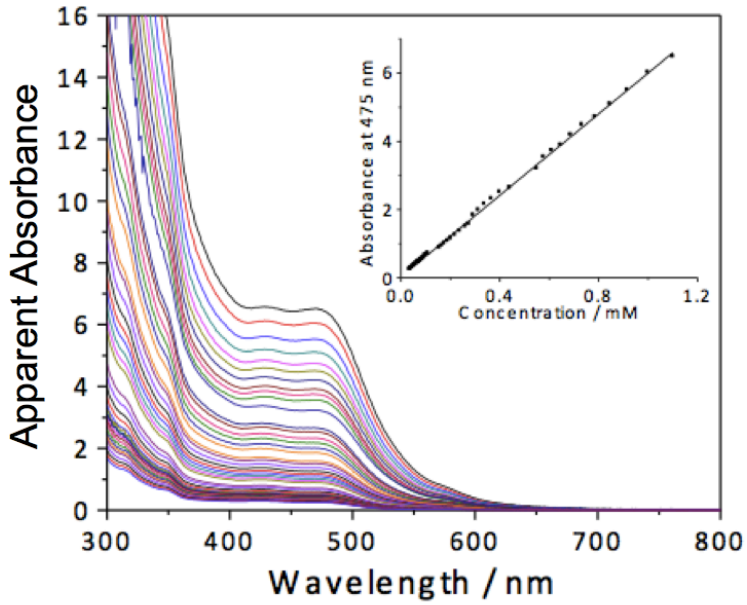

Figure S2. Concentration-dependent UV–vis absorption spectra of **1** in THF (from 4 × 10^{-5} M to 1.1 × 10^{-3} M) with increasing concentration at 298 K. The inset shows the apparent absorbance at 475 nm as a function of concentration of complex **1**. The apparent absorbance values have been obtained by correcting to a 1-cm path length equivalence.

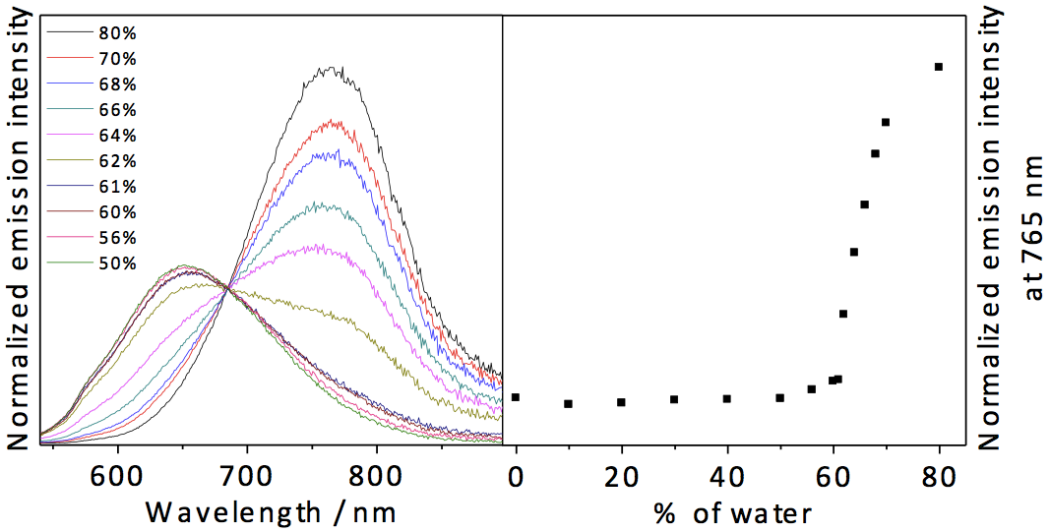

Figure S3. (Left) Emission spectral changes of **1** in THF normalized at 685 nm upon increasing water content from 50 to 80 %. (Right) The corresponding plot of normalized emission intensity monitored at 765 nm against the changes in water content, illustrating solvent composition of *ca.* 62 % water/THF is required to trigger the ^{3}MMLCT emission band, which is consistent with the UV–vis absorption study.

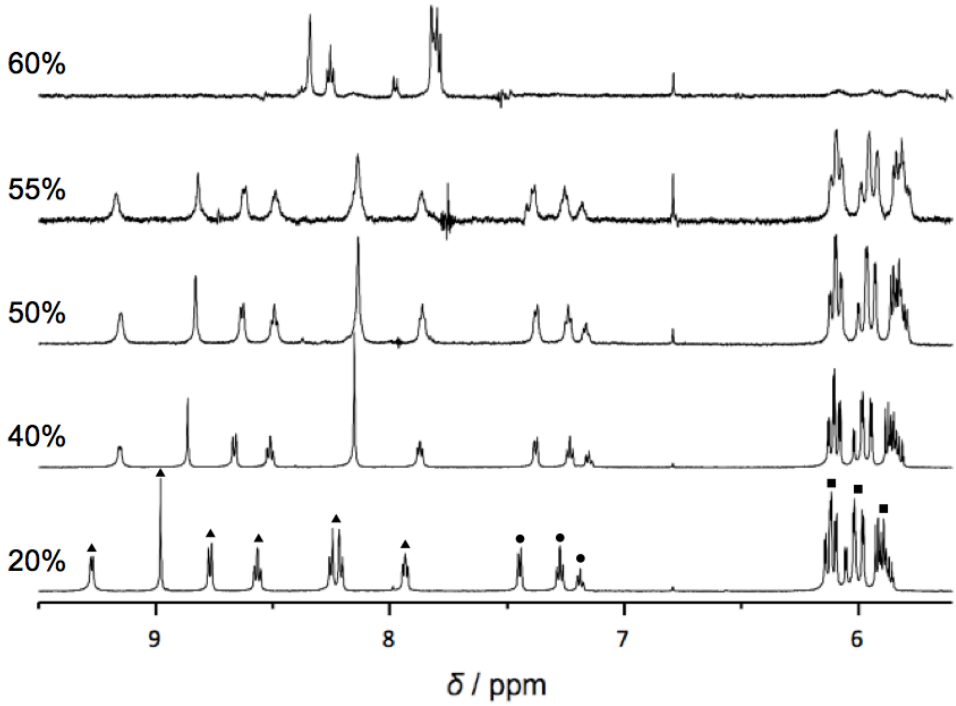

Figure S4. Solvent composition dependent ^{1}H NMR spectra of **1** in D_2O–[D_8]THF (v/v). Proton signals correspond to the terpyridine moiety (▲), phenyl ring (●), and the vinyl groups on the POSS moieties (■).

Table S4 Dynamic light scattering data of **1**

Complex	Medium (T / K)	Hydrodynamic diameter (D_H / nm)
1	30% water/THF (v/v, 298)	3.6,[a] 709.1[b]
	70% water/THF (v/v, 298)	113.7,[c] 866.6
	40% hexane/THF (v/v, 298)	781.2

[a]Small aggregates (probably dimeric to tetrameric species).
[b]The size is slightly larger than the TEM findings, probably due to shrinkage of the structures by loss of solvent during the drying process for TEM measurements.
[c]This is due to small rod fragments, consistent with the TEM finding.

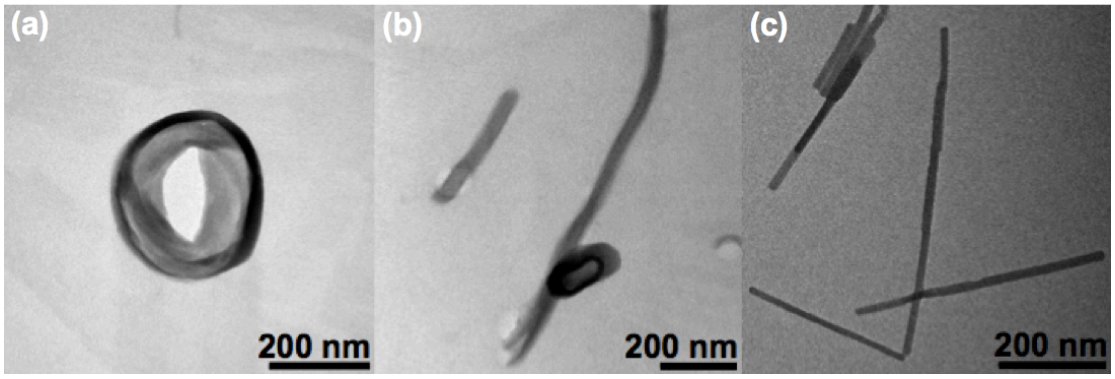

Figure S5. TEM images of the superstructures prepared from **1** (2 x 10^{-4} M) in (a) 30 %; (b) 50 %; (c) 70 % (v/v) water–THF mixture, showing the morphological transformation from (a) nanorings to (c) nanorods through an intermediate state with the (b) coexistence of both nanorings and nanorods.

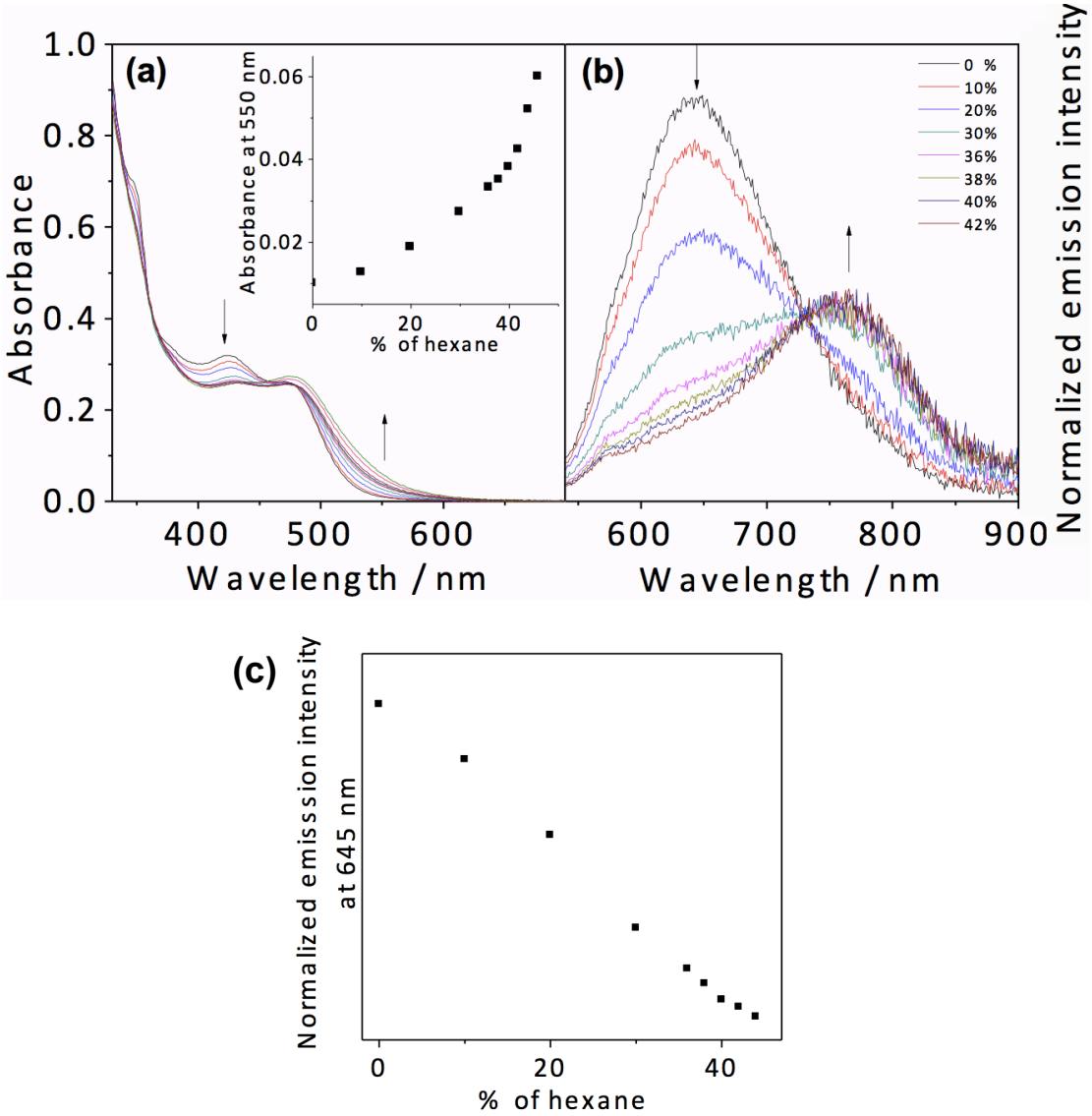

Figure S6. (a) UV–Vis absorption spectra of **1** in THF with increasing hexane content from 0 to 46 %. (b) The corresponding corrected emission spectral changes normalized at 730 nm upon increasing the hexane composition from 0 to 42 %. (c) The corresponding plot of normalized emission intensity monitored at 645 nm against the changes in hexane content.

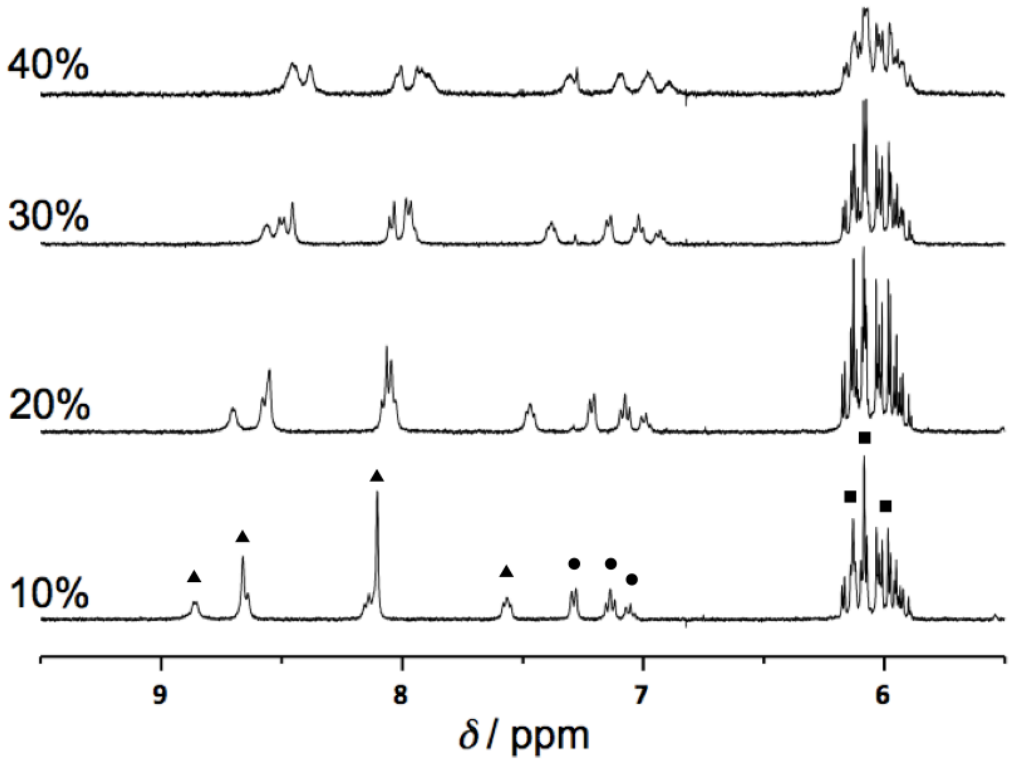

Figure S7. Solvent composition dependent ^{1}H NMR spectra of **1** in [D_{14}]hexane–[D_8]THF (v/v). Proton signals correspond to the terpyridine moiety (▲), phenyl ring (●), and the vinyl groups on the POSS moieties (■). The upfield shift and signal broadening corresponding to the terpyridine and POSS moieties reveal the presence of molecular interactions in the self-assembly process at increasing hexane content.

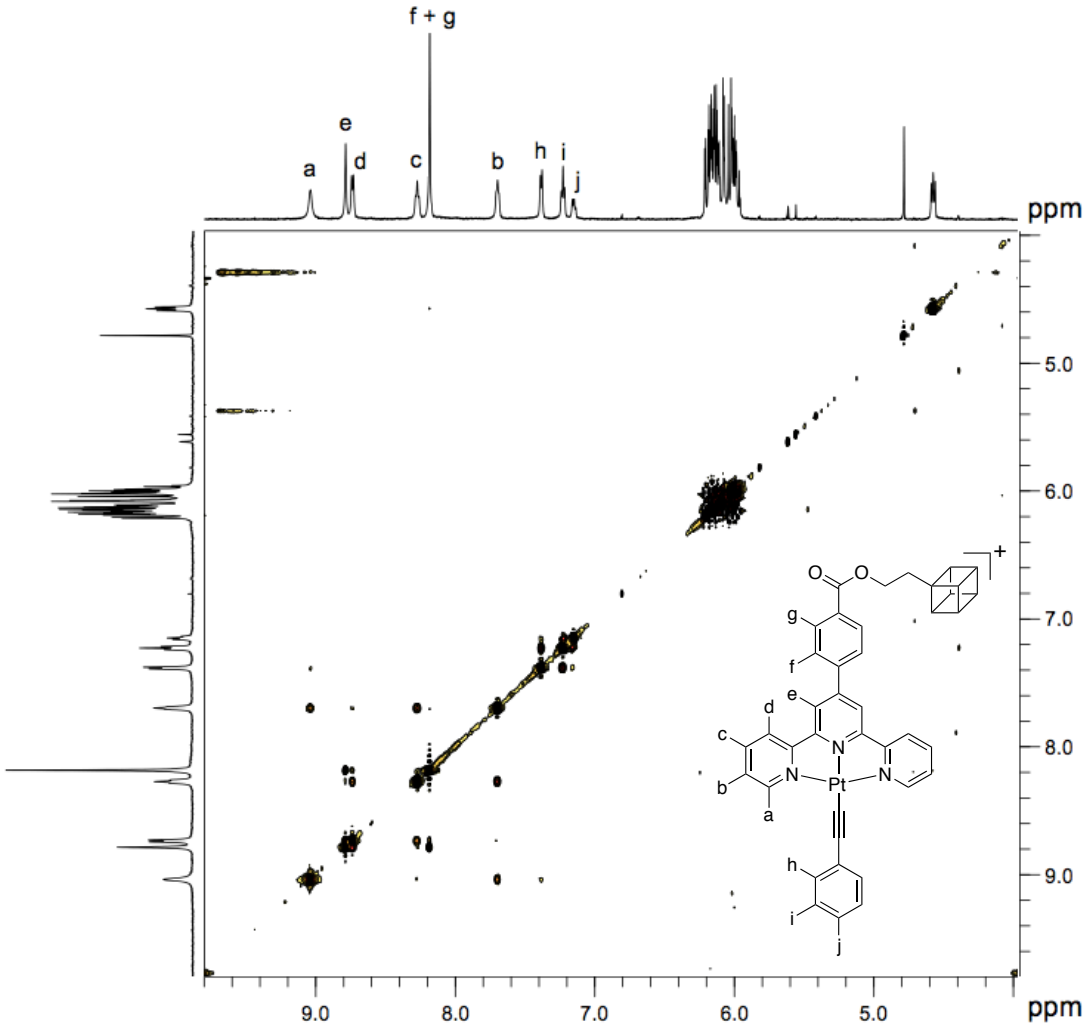

Figure S8. ^{1}H–^{1}H NOESY spectrum of **1** in [D_8]THF. Terpyridine and phenyl protons are assigned accordingly.

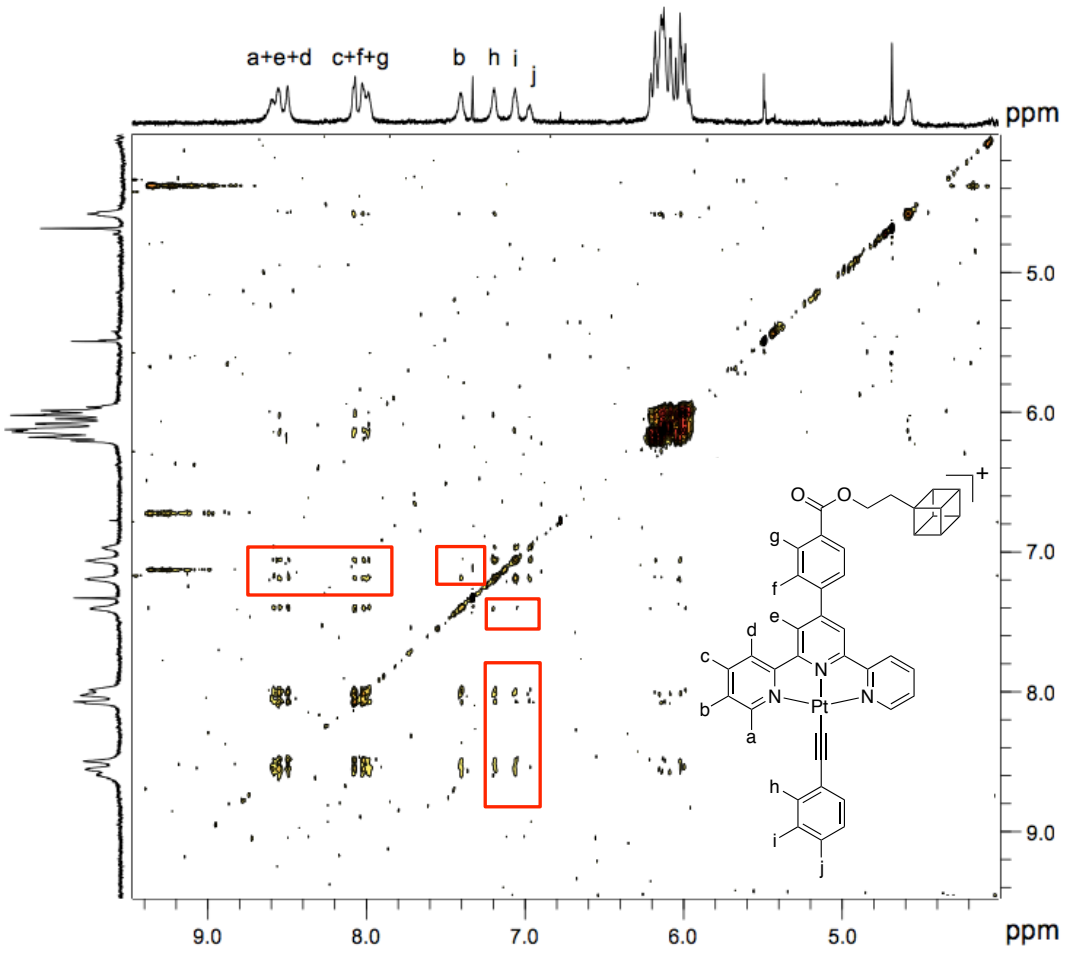

Figure S9. ^{1}H–^{1}H NOESY spectrum of **1** in 40% [D_{14}]hexane–[D_8]THF. Cross-peaks between the phenyl protons (h–j) and the terpyridine signals (a–g) with NOE interactions were observed (red boxes), suggesting the possible adoption of a head-to-tail packing conformation in THF–hexane media.

References

1 Feher, F. J.; Wyndham, K. D.; Baldwin, R. K.; Soulivong, D.; Lichtenhan, J. D.; Ziller, J. W. *Chem. Commun.* **1999,** 1289.

2 Manner, J V. W.;. Mayer, M. *J. Am. Chem. Soc.* **2009,** 9874.

3 a) Yip, H. K.; Cheng, L. K.; Cheung, K. K.; Che, C. M. *J. Chem. Soc. Dalton Trans.*, **1993,** 2933; b) Bailey, J. A.; Hill, M. G.; Marsh, R. E.; Miskowski, V. M.; Schaefer, W. P.; Gray, H. B. *Inorg. Chem.* **1995,** 34, 4591.

4 a) Tam, A. Y. Y.; Wong, K. M. C.; Wang, G.; Yam, V. W. W. *Chem. Commun.* **2007**, 2028; b) Lu, W.; Law, Y. C.; Han, J.; Chui, S. S. Y.; Ma, D. L.; Zhu, N.; Che, C. M. *Chem. Asian J.* **2008,** 3, 59.

5. Bruker AXS Inc. APEX, Madison, Wisconsin, USA, **2010**.

6 Sheldrick, G. M. SADABS, Empirical Absorption Correction Program. Göttingen University, Göttingen, Germany, **2008**.

7 Sheldrick, G. M. *Acta Crystallogr. Sect A* **2008**, 64, 112.